Size-Tunable Synthesis of SiO_2 Nanotubes via a Simple In Situ Templatelike Process

Guozhen Shen,* Yoshio Bando, and Dmitri Golberg

Nanoscale Materials Center, National Institute for Materials Science (NIMS), Namiki 1-1, Tsukuba, Ibaraki 305-0044, Japan

Received: July 18, 2006; In Final Form: September 13, 2006

SiO_2 nanotubes with tunable diameters and lengths have been successfully synthesized via a simple in situ templatelike process by thermal evaporation of SiO, ZnS, and GaN in a vertical induction furnace. The structure and morphologies were systematically investigated using X-ray diffraction, scanning electron microscopy, transmission electron microscopy, and energy-dispersive X-ray spectrometry. Studies found that both the diameters and lengths of the SiO_2 nanotubes can be effectively tuned by simply changing the reaction temperatures. The range of changes was from 30 nm (diameter) and several hundred micrometers (length) at 1450 °C to 100 nm (diameter) and 2−10 micrometers (length) at 1300 °C. Varying some other experimental parameters results in the formation of additional SiO_2-based nanostructures, such as core−shell ZnS−SiO_2 nanocables, ZnS nanoparticle filled SiO_2 nanotubes, and fluffy SiO_2 spheres. Based on the observations, an in situ templatelike process was proposed to explain the possible growth mechanism.

Introduction

Following the discovery of carbon nanotubes,[1] one-dimensional (1-D) inorganic nanotubes have become symbols of the new and fast developing research area of nanotechnology due to many significant potential applications.[2−7] Numerous methods have been developed to synthesize nanotubes with the layered or pseudo-layered structures as well as nonlayered nanotubes.[2−20] The prepared nanotubes include boron nitride, metal dichalcogenides, metal dihalides, metal oxides and hydroxides, metal borates, metals, silicon, metal nitrides, and metal phosphides, etc.

Among various nanotubes, silica nanotubes (SiO_2 nanotubes) have received significant attention due to their room-temperature light-emission characteristics in the visible range, a possible usage for hosting materials in bioanalysis and bioseparation and potential applications in optoelectronic nanodevices. Since Harada and Adachi reported the synthesis of silica nanotubes in 2000 by a surfactant-mediated method, several techniques have been developed to prepare silica nanotubes.[21−25] For example, Jang[21] et al. reported the synthesis of size-tunable silica nanotubes using a reverse microemulsion-mediated sol−gel method. Nesper synthesized silica nanotubes with a high aspect ratio using fibers of vanadium oxide hydrate as the templates. Mayer used a templated surface sol−gel technique to get silica nanotubes. Wang synthesized silica nanotubes using zinc oxide nanowires as the removable templates. Our groups reported the synthesis of ultralong silica nanotubes using an indium-assisted vapor phase process.

In this work, we reported the synthesis of size-tunable silica nanotubes via a simple in situ templatelike process by thermal evaporation of a mixture of SiO, ZnS and GaN in a vertical induction furnace. In this process, both the diameters and lengths of the silica nanotubes can be easily tuned by changing the reaction temperatures.

Experimental Section

SiO_2 nanotubes were synthesized in a vertical induction furnace as described in detail in the literature,[26] which consists of a fused-quartz tube and an induction-heated cylinder made of high purity graphite coated with a carbon fiber thermo-insulating layer. The furnace has an inlet on its top and one outlet on its base, respectively. A graphite crucible, containing a mixture of ZnS (0.1 g), SiO (1 g), and GaN (0.1 g) powders, was placed at the center cylinder zone. After evacuation of the quartz tube to ~100 Pa, pure Ar was introduced into the furnace through the inlet at the base, which was maintained at a flow rate of 200 sccm. The furnace was rapidly heated and kept at 1450 °C or 1300 °C for about 1 h. After the reaction was terminated and the furnace cooled to room temperature, the collected products were characterized using powder X-ray diffraction (XRD, RINT 2200) with Cu Kα radiation, scanning electron microscopy (SEM, JSM-6700), and transmission electron microscopy (TEM, JEM-3000F) equipped with an energy-dispersive X-ray spectrometer (EDS).

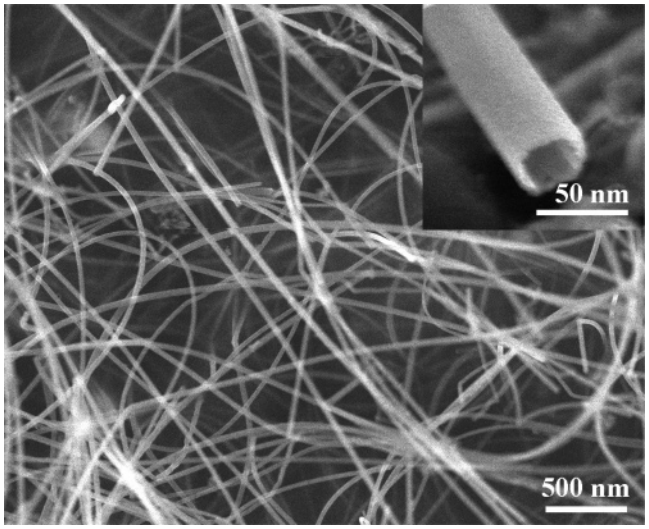

Figure 1. SEM image of the obtained SiO_2 nanotubes with diameters of ~30 nm synthesized at 1450 °C.

10.1021/jp064537w CCC: $33.50
Published on Web 10/24/2006

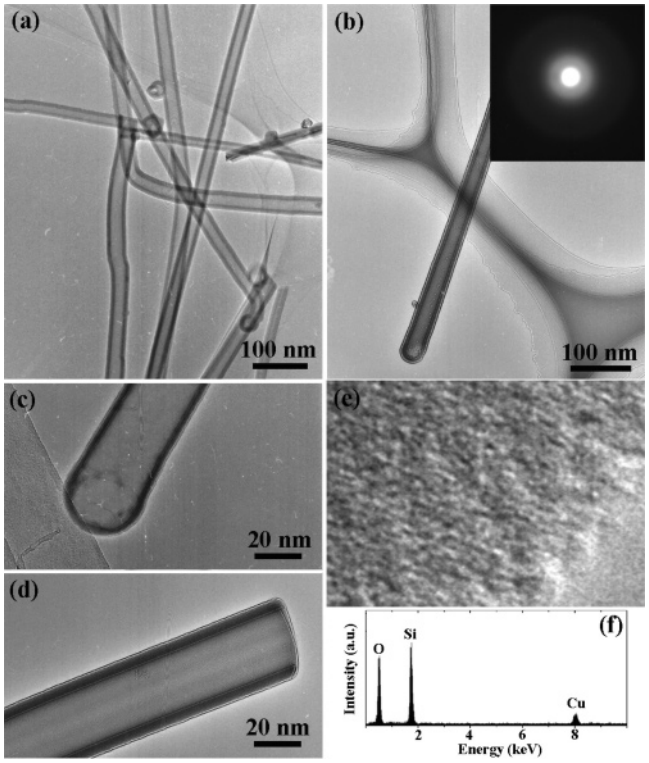

Figure 2. (a) TEM image of several SiO_2 nanotubes with typical diameters of ~30 nm. (b) TEM image of a single SiO_2 nanotube. (c, d) TEM images of the closed and open tips of the synthesized SiO_2 nanotubes. (e) HRTEM image and (f) EDS spectrum of a SiO_2 nanotube.

Results and Discussion

Structure and Composition. After reaction, the powder was collected from the inner wall of the crucible and checked using XRD. The XRD spectrum shows a broad peak at $2\theta = 20-30°$, indicating only amorphous materials within the product. EDS studies reveal the composition of Si:O = 1:2, thus the formation of amorphous SiO_2 (see below) is documented.

SiO_2 Nanotubes with a Diameter of ~30 nm Synthesized at 1450 °C. Figure 1 shows the SEM image of the product obtained at 1450 °C. It displays the formation of large scale 1-D wire-like nanostructures with lengths up to several hundred micrometers. Increasing the magnification reveals that they are SiO_2 nanotubes with uniform diameters of about 30 nm (inset in Figure 1).

The SiO_2 nanotubes were further characterized using TEM. Figures 2a and 2b are the TEM images of the synthesized SiO_2 nanotubes. Typical nanotubes have smooth surfaces, round cross sections for both their interiors and exteriors, and diameters of about 30 nm in accordance to the SEM results. From these images, we can also see that the SiO_2 nanotubes have a very thin wall thickness of about 5 nm. All the SiO_2 nanotubes have one round closed end and one open end as shown in Figures 2c and 2d. The corresponding selected area electron diffraction (SAED) pattern is shown in Figure 2b inset. The halolike SAED pattern shows that the synthesized SiO_2 nanotubes are in the amorphous states. Figure 2e shows the HRTEM image of a single SiO_2 nanotube. No lattice fringe could be observed for the nanotube also indicates its amorphous state. Figure 2f is a typical EDX spectrum taken from the SiO_2 nanotube. Only Si and O peaks are present in the spectrum with the atomic ratio of ~0.5, confirming these nanotubes are amorphous SiO_2 nanotubes. The peak at about 8 keV comes from the copper foils used for TEM analysis.

SiO_2 Nanotubes with Diameter of ~100 nm Synthesized at 1300 °C. During our experiments, it was found that the diameters of the obtained SiO_2 nanotubes can be easily tuned by changing the reaction temperatures. Figures 3a and 3b show the SEM images of the product obtained at 1300 °C, which

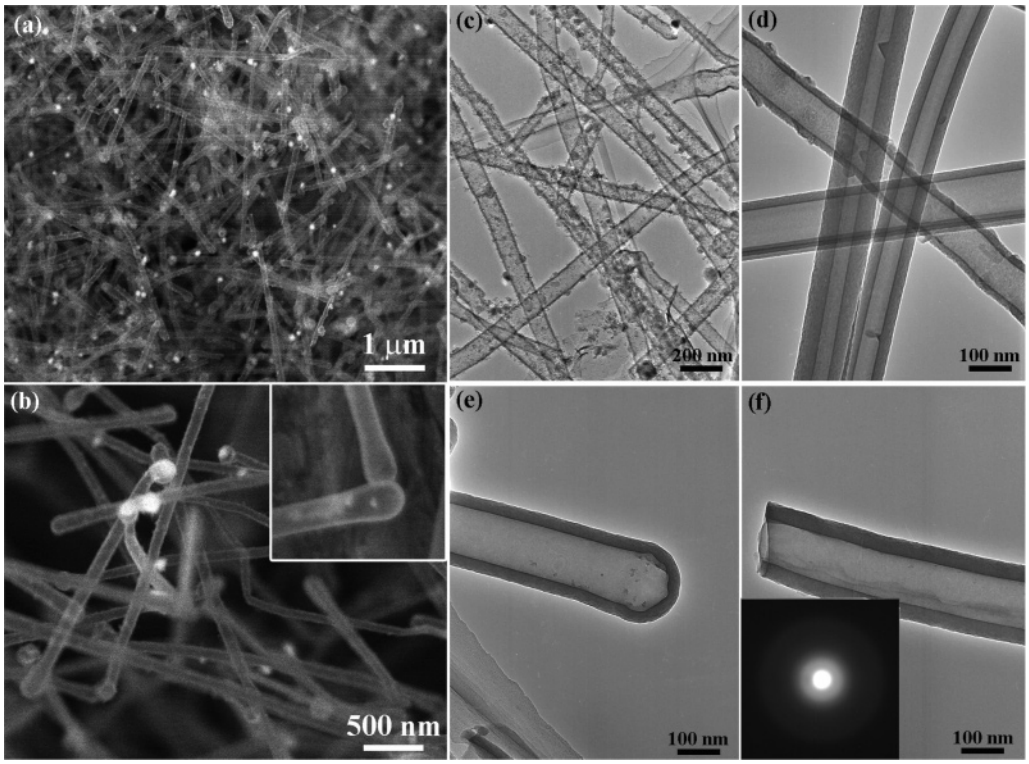

Figure 3. (a, b) SEM images of the synthesized SiO_2 nanotubes with diameters of ~100 nm synthesized at 1300 °C. (c) TEM image of the obtained SiO_2 nanotubes. (d) TEM image of the SiO_2 nanotubes after acid treatment. (e, f) TEM images of the closed tip and open tip of a SiO_2 nanotube.

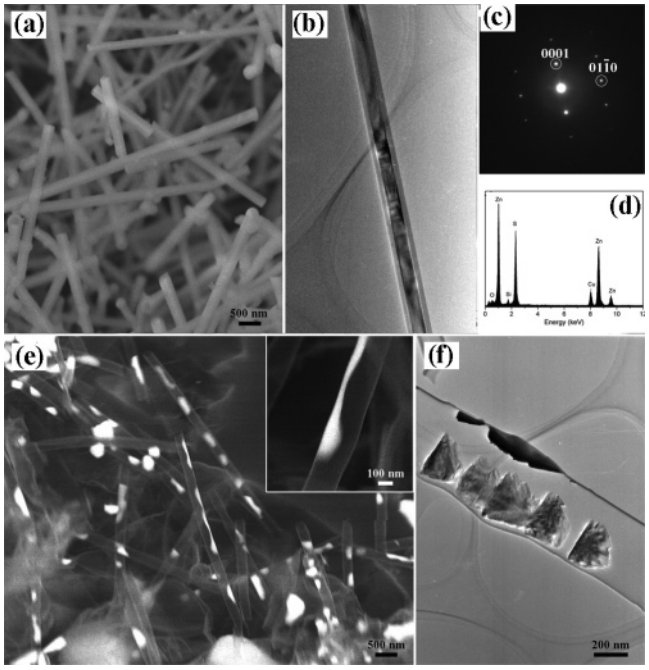

Figure 4. (a) SEM image and (b) TEM image of the synthesized coaxial ZnS/SiO_2 nanocables. (c) SAED pattern of the nanocable in part b. (d) EDS pattern taken from the inner nanowire. (e) SEM image and (f) TEM image of SiO_2 nanotubes partially filled with ZnS.

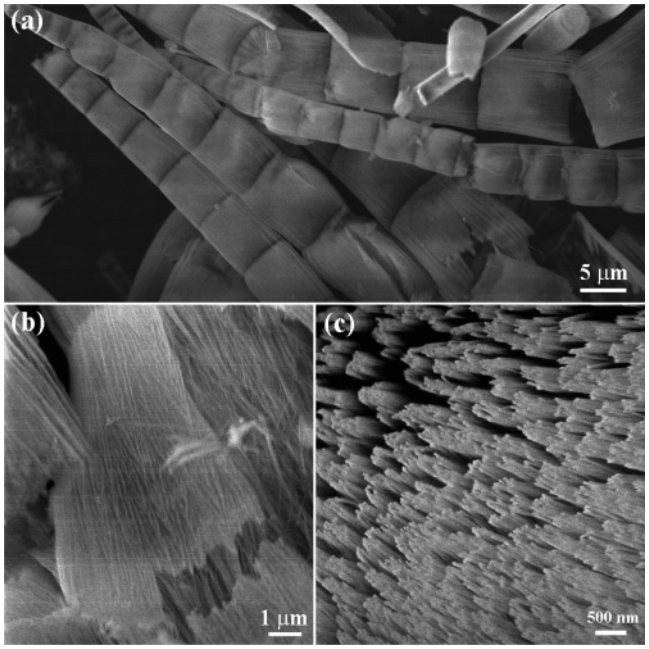

Figure 5. SEM images of the SiO_2 microrods obtained without the use of ZnS, which are composed of highly aligned SiO_2 nanowires.

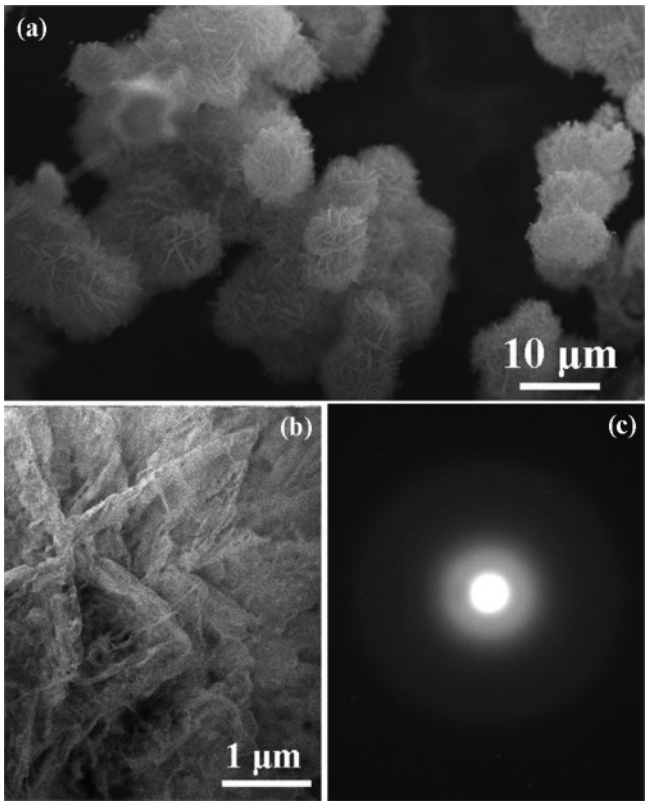

Figure 6. (a, b) SEM images with different magnifications of the fluffy SiO_2 spheres synthesized in the absence of GaN. (c) The corresponding SAED pattern of the fluffy SiO_2 sphere.

also indicates the formation of large-scale 1-D nanotube structures at this temperature. However, high-magnification SEM images show that the diameters and lengths of these structures at 1300 °C change dramatically compared with those obtained at 1450 °C.

Figure 3c is the TEM image of the products obtained at 1300 °C. It indicates the formation of hollow SiO_2 nanotubes with outer diameters of ∼100 nm. The wall thickness of these nanotubes can be derived from the high-magnifcation TEM images in Figure 3d. It shows the wall thickness in the range of 15−30 nm. Similar to those SiO_2 nanotubes obtained at 1450 °C, SiO_2 nanotubes synthesized at 1300 °C also have one closed tip and one open tip, which are demonstrated in Figures 3e and 3f. The SAED pattern inset in Figure 3f also shows the amorphous states of these nanotubes. Besides the straight SiO_2 nanotubes, some interesting tubular SiO_2 nanostructures, such as "H"-type and "Y"-type, were also obtained under the present experimental conditions (Supporting Information).

Effect of ZnS Concentration. All the above discussions have confirmed that the present method is an efficient process to produce size-tunable SiO_2 nanotubes on a large scale. It was also found that the final products are quite sensitive to the concentration of ZnS in the source materials. Figure 4a shows the SEM image of the product when 0.35 g of ZnS powder was used. From this image, it can be clearly seen that 1-D nanowires are obtained on a large scale. The corresponding TEM image in Figure 4b showing clear contrast variations between the outer part and inner part, indicates that these 1-D nanowires are novel core-sheath heterostructures. The inner ZnS nanowires have diameters of 50−100 nm and the thickness of the outer SiO_2 ranging from about 5 nm to 70 nm. Figure 4c shows the SAED pattern taken from the core of the core−shell structure shown in Figure 4b. The pattern can be indexed to wurtzite ZnS along the [100] zone axis, which has the growth direction along the [0001] plane. The EDS spectrum of the core nanowire generated by a nanobeam is shown in Figure 4d. It shows the peaks of Zn and S elements with a Zn/S molar ratio close to the ZnS stoichiometry, indicating that the inner nanowire is ZnS.

Another kind of 1-D product was obtained when 0.2 g of ZnS powder was used, and a typical SEM image is shown in Figure 4e. It clearly shows the formation of partially ZnS-filled SiO_2 nanotubes. Typical partially ZnS-filled SiO_2 nanotube has a length of several micrometers and diameter of 100−350 nm. Figure 4f is the TEM image of a single partially ZnS-filled SiO_2 nanotube with diameter of about 300 nm which confirms the

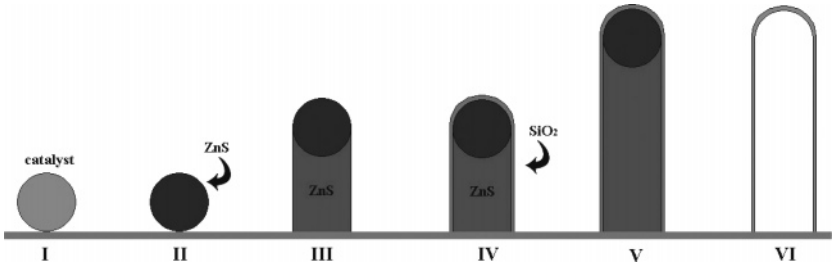

Figure 7. Schematic illustration of the formation of SiO_2 nanotubes via an in situ templatelike process. (I) Formation of liquid-Ga droplets. (II) Condensation of ZnS on Ga droplets. (III) Simultaneous growth of ZnS nanowires. (IV) Deposition of SiO_2 on the surface of ZnS nanowires. (V) Formation of coaxial ZnS/SiO_2 hetero-nanowires. (VI) Formation of SiO_2 nanotubes.

TABLE 1: Relationships of the Products and the Source Materials and Reaction Temperatures

material	T (°C)	product
GaN + SiO	1300	SiO_2 micro-rods composed of aligned SiO_2 nanowires
GaN + SiO + ZnS (SiO:ZnS = 10:1)	1450	SiO_2 Nanotubes (D: 30 nm, L: several hundred micrometers)
	1300	SiO_2 Nanotubes (D: 100 nm, L: several to tens micrometers)
GaN + SiO + ZnS (SiO:ZnS = 5:1)	1300	partially ZnS filled SiO_2 nanotubes
GaN + SiO + ZnS (SiO:ZnS = 20:7)		coaxial ZnS/SiO_2 nanocables
GaN + SiO + ZnS (SiO:ZnS < 2:1)	1300−13 50	hierarchical ZnS/SiO_2 nanowire heterostructures
SiO + ZnS	1300	fluffy SiO_2 spheres

SEM results (see also Supporting Information). When increased amounts of ZnS are used in the experiments, hierarchical ZnS/SiO_2 nanowire heterostructures are obtained instead of 1-D nanowires according to our previous report.[27]

In the experiments, when the amount of ZnS was decreased to lower than 0.1 g or when no ZnS was used, only Ga-attached SiO_2 microrods are obtained as shown in Figure 5a. Higher magnification SEM images shown in Figures 5b and 5c depict that the as-obtained SiO_2 microrods are composed of highly aligned amorphous SiO_2 nanowires with very high density (Supporting Information). Similar phenomena were also observed by Yang et al.[28]

Growth Mechanism. During the synthetic process, GaN plays an important role in the thermal evaporation of SiO and ZnS to generate SiO_2 nanotubes. Without the use of GaN and when all the other experimental parameters are kept constant, only fluffy SiO_2 spheres are obtained. Figures 6a and 6b show the SEM images of the product obtained by thermal evaporation of only ZnS and SiO at 1300 °C. They reveal the formation of many fluffy spheres typically ranging from 1 to 10 μm in diameter. Each fluffy sphere consists of numerous nanowires of several tens to one hundred nanometers in diameter. The formation of fluffy spheres was further confirmed using TEM analysis (Supporting Information). It shows the arrangement of nanowires into spherical structure as the SEM result. The corresponding SAED pattern shown in Figure 6c confirms its amorphous state, and EDS analysis reveals that these fluffy spheres are pure SiO_2 product. Table 1 shows the effect of experiments on the final products, illustrating the relationships of the products, source mateials, and reaction temperatures.

Based on the above analyses, an in situ templatelike process was proposed to explain the formation of SiO_2 nanotubes, and the whole process can be schematically illustrated in Figure 7. At high reaction temperature, GaN decomposes to Ga and the newly formed Ga may be in the form of small-sized liquid clusters (the decomposition of GaN at high temperature is confirmed by the observation of many metallic Ga spheres remained in the crucible after reaction). The Ga clusters are then transported by Ar gas to the low temperature region, where they deposit in the form of liquid droplets on the inner wall of the graphite crucible (I). The as-formed Ga droplets are energetically favored sites for the absorption of incoming ZnS vapors generated in the system (II). Once becoming supersaturated, ZnS segregates and gives rise to the 1-D growth of ZnS nanowires (III). With the increase of processing temperature, thermal decomposition of the SiO powder results in the formation of Si vapors which are easily oxidized by the residual O_2, or the unavoidable negligible leakage of O_2 into the reaction system, to SiO_2, which is transported by the Ar gas and deposits on the surface of newly formed ZnS nanowires (IV), resulting in ZnS/SiO_2 hetero-nanowires (V). Due to the high temperature, the inner ZnS nanowires are evaporated, and finally hollow SiO_2 nanotubes are formed (VI).

Conclusion

In conclusion, we developed a simple thermal evaporation process for the synthesis of SiO_2 nanotubes using in situ-formed ZnS nanowires as the templates. Both the diameters and lengths of the SiO_2 nanotubes can be effectively tuned through only changing the evaporation temperature. Careful investigations of the experimental parameter influence on the final product morphologies revealed that coaxial ZnS/SiO_2 hetero-nanowires, partially filled SiO_2 nanotubes, and fluffy SiO_2 spheres may also form. The results suggest that the present method is not only an efficient approach to fabricate pure SiO_2 nanotubes with tunable sizes but also a smart way to protect ZnS nanowires from oxidation using SiO_2 surface coatings and/or to fabricate complex SiO_2-based structures on a large scale.

Acknowledgment. We thank Y. Uemura for advice during material synthesis and K. Kurashima for technical assistance in TEM work.

Supporting Information Available: TEM images of H-type and Y-type SiO_2 nanotubes, EDS spectrum taken from the partially ZnS-filled SiO_2 nanotube, SEM images showing the attached Ga catalyst, high-magnification SEM image of highly aligned SiO_2 nanowires, and SEM images and SAED pattern of fluffy SiO_2 spheres. This material is available free of charge via the Internet at http://pubs.acs.org.

References and Notes

(1) Iijima, S. *Nature (London)* **1991**, *354*, 56.

(2) Dai, H. J.; Wang, E. W.; Lu, Y. Z.; Fan, S. S.; Lieber, C. M. *Nature (London)* **1995**, *375*, 769.

(3) (a) Chopra, N. G.; Luyken, R. J.; Cherrey, K.; Crespi, V. H.; Cohen, M. L.; Luoise, S. G.; Zittl, A. *Science* **1995**, *269*, 966. (b) Tenne, R.; Margulis, L.; Genut, M.; Hodes, G. *Nature* **1992**, *360*, 444.

(4) (a) Hacohen, Y. R.; Grunbaum, E.; Tenne, R.; Sloan, J.; Hutchson, J. L. *Nature (London)* **1998**, *395*, 336. (b) Spahr, M. E.; Bitterli, P.; Nesper, R.; Müller, M.; Krumeich, F.; Nissen, U. *Angew. Chem., Int. Ed.* **1998**, *37*, 7, 1263. (c) Feldman, Y.; Wasserman, E.; Srolovitz, D. J.; Tenne, R. *Science* **1995**, *267*, 222.

(5) (a) Nath, M.; Rao, C. N. R. *J. Am. Chem. Soc.* **2001**, *123*, 4841. (b) Ajayan, P. M.; Stephan, O.; Redlich, P.; Colliex, C. *Nature (London)* **1995**, *375*, 564.

(6) (a) Hutleen, J. C.; Jirage, K. B.; Martin, C. R. *J. Am. Chem. Soc.* **1998**, *120*, 6603. (b) Mayers, B.; Xia, Y. N. *Adv. Mater.* **2002**, *14*, 279. (c) Nakamura, H.; Matsui, Y. *J. Am. Chem. Soc.* **1995**, *117*, 2651.

(7) (a) Xu, A. W.; Fang, Y. P.; You, L. P.; Liu, H. Q. *J. Am. Chem. Soc.* **2003**, *125*, 1494. (b) Li, Y.; Wang, J.; Deng, Z.; Wu, Y.; Sun, X.; Yu, D.; Yang, P. D. *J. Am. Chem. Soc.* **2001**, *123*, 9904. (c) Shen, G. Z.; Bando, Y.; Zhi, C. Y.; Golberg, D. *J. Phys. Chem. B* **2006**, *110*, 10714.

(8) (a) Ma, R. Z.; Bando, Y.; Golberg, D.; Sato, T. *Angew. Chem., Int. Ed.* **2003**, *42*, 1836. (b) Hu, J. Q.; Bando, Y.; Liu, Z. W.; Zhan, J. H.; Golberg, D.; Sekiguchi, T. *Angew. Chem., Int. Ed.* **2004**, *43*, 63.

(9) (a) Goldberger, J.; He, R. R.; Zhang, Y. F.; Lee, S.; Yan, H. Q.; Choi, H. J.; Yang, P. D. *Science* **2003**, *422*, 599. (b) Yang, P. D. *Abstr. Pap. Am. Chem. Soc.* **2004**, *227*, U248. (c) Remskar, M. *Adv. Mater.* **2004**, *16*, 1407.

(10) (a) Li, Y. B.; Bando, Y.; Golberg, D. *Adv. Mater.* **2005**, *17*, 1401. (b) Yin, L. W.; Bando, Y.; Zhu, Y. C.; Li, M. S.; Tang, C. C.; Golberg, D. *Adv. Mater.* **2005**, *17*, 213.

(11) (a) Tang, C. C.; Bando, Y.; Golberg, D.; Ma, R. Z. *Angew. Chem., Int. Ed.* **2005**, *44*, 576. (b) Yin, L. W.; Bando, Y.; Golberg, D.; Li, M. S. *Adv. Mater.* **2004**, *16*, 1833. (c) Yin, L. W.; Bando, Y.; Golberg, D.; Li, M. S. *Appl. Phys. Lett.* **2004**, *85*, 3869.

(12) (a) Yu, S. F.; Welp, U.; Hua, L. Z.; Rydh, A.; Kwok, W. K.; Wang, H. H. *Chem. Mater.* **2005**, *17*, 3445. (b) Yang, J.; Liu, Y. C.; Lin, H. M.; Chen, C. C. *Adv. Mater.* **2004**, *16*, 713.

(13) (a) Yin, L. W.; Bando, Y.; Zhu, Y. C.; Golberg, D.; Li, M. S. *Adv. Mater.* **2004**, *16*, 929. (b) Yin, L. W.; Bando, Y.; Zhu, Y. C.; Golberg, D.; Li, M. S. *Appl. Phys. Lett.* **2004**, *84*, 3912.

(14) Zhan, J. H.; Bando, Y.; Hu, J. Q.; Golberg, D. *Inorg. Chem.* **2004**, *43*, 2462.

(15) (a) Li, Y. B.; Bando, Y.; Golberg, D.; Uemura, Y. *Appl. Phys. Lett.* **2003**, *83*, 3999. (b) Hu, J. Q.; Bando, Y.; Golberg, D.; Liu, Q. L. *Angew. Chem., Int. Ed.* **2003**, *42*, 3493.

(16) (a) Li, Y. B.; Bando, Y.; Golberg, *Adv. Mater.* **2003**, *15*, 1294. (b) Tang, C. C.; Bando, Y.; Sato, T.; Kurashima, K. *Chem. Commun.* **2002**, 1290. (c) Ma, R. Z.; Bando, Y.; Sato, T.; Kurashima, *Chem. Mater.* **2001**, *13*, 2965.

(17) (a) Wang, Y.; Lee, J. Y.; Zeng, H. C. *Chem. Mater.* **2005**, *17*, 3899. (b) Li, X. X.; Cheng, F. Y.; Guo, B.; Chen, J. *J. Phys. Chem. B* **2005**, *109*, 14017.

(18) (a) Jia, C. J.; Sun, L. D.; Yan, Z. G.; You, L. P. Han, X. D.; Pang, Y. C.; Zhang, Z.; Yan, C. H. *Angew. Chem., Int. Ed.* **2005**, *44*, 4328. (b) Sehayek, T.; Lahav, M.; Popovitz-Biro, R.; Vaskevich, A.; Rubinstein, I. *Chem. Mater.* **2005**, *17*, 3743. (c) Liu, Z. Q.; Zhang, D. H.; Han, S.; Li, C.; Lei, B.; Lu, W. G.; Fang, J. Y.; Zhou, C. W. *J. Am. Chem. Soc.* **2005**, *127*, 6.

(19) (a) Park, T. J.; Mao, Y. B.; Wong, S. S. *Chem. Commun.* **2004**, 2708. (b) Wang, J. X.; Wen, L. X.; Wang, Z. H.; Wang, M.; Shao, L.; Chen, J. F. *Script. Mater.* **2004**, *51*, 1035. (c) Qu, L. T.; Shi, G. Q.; Wu, X. F.; Fan, B. *Adv. Mater.* **2004**, *16*, 1200.

(20) (a) Guo, L.; Liu, C. M.; Wang, R. M.; Xu, H. B.; Wu, Z. Y.; Yang, S. *J. Am. Chem. Soc.* **2004**, *126*, 4530. (b) Wang, X.; Zhuang, J.; Chen, J.; Zhou, K. B.; Li, Y. D. *Angew. Chem., Int. Ed.* **2004**, *43*, 2017.

(21) (a) Harada, M.; Adachi, M. *Adv. Mater.* **2000**, *12*, 839. (b) Jang, J. S.; Yoo, H. S. *Adv. Mater.* **2004**, *16*, 799. (c) Wang, L. Z.; Tomura, S.; Ohashi, F.; Maeda, M.; Suzuki, M.; Inukai, K. *J. Mater. Chem.* **2001**, *11*, 1465.

(22) (a) Zygmunt, J.; Krumeich, F.; Nesper, R. *Adv. Mater.* **2003**, *15*, 1538. (b) Li, Y. B.; Bando, Y.; Golberg, D. *Adv. Mater.* **2004**, *16*, 37.

(23) (a) Chen, Y. J.; Xue, X. Y.; Wang, T. H. *Nanotechnology* **2005**, *16*, 1978. (b) Wang, Z. L.; Gao, R. P.; Gole, J. L.; Stout, J. D. *Adv. Mater.* **2000**, *12*, 1938.

(24) (a) Zhang, M.; Ciocan, E.; Bando, Y.; Wada, K.; Cheng, L. L.; Pirouz, P. *Appl. Phys. Lett.* **2002**, *80*, 491. (b) Yin, Y. D.; Lu, Y.; Sun, Y. G.; Xia, Y. N. *Nano Lett.* **2002**, *2*, 427. (c) Fan, R.; Wu, Y.; Li, D.; Yue, M.; Majumdar, A.; Yang, P. D. *J. Am. Chem. Soc.* **2003**, *125*, 5254.

(25) (a) Hu, J. Q.; Meng, X. M.; Jiang, Y.; Lee, C. S.; Lee, S. T. *Adv. Mater.* **2003**, *15*, 70. (b) Yao, B. D.; Fleming, D.; Morris, M. A.; Lawrence, S. E. *Chem. Mater.* **2004**, *16*, 4851.

(26) (a) Shen, G. Z.; Bando, Y.; Liu, B. D.; Tang, C. C.; Huang, Q.; Golberg, D. *Chem.—Eur. J.* **2006**, *12*, 2987. (b) Han, W.; Bando, Y.; Kurashima, K.; Sato, Y. *Appl. Phys. Lett.* **1998**, *73*, 3085.

(27) Shen, G. Z.; Bando, Y.; Tang, C. C.; Golberg, D. *J. Phys. Chem. B* **2006**, *110*, 7199.

(28) Zheng, B.; Wu, Y. Y.; Yang, P. D.; Liu, J. *Adv. Mater.* **2001**, *14*, 122.